Nonuniversal gaugino masses and muon g-2

Ilia Gogoladze, Fariha Nasir, Qaisar Shafi, and Cem Salih Ün

Nonuniversal Gaugino Masses and Muon $g-2$

Ilia Gogoladze[1], Fariha Nasir[2], Qaisar Shafi[3] and Cem Salih Ün[4]

Bartol Research Institute, Department of Physics and Astronomy,
University of Delaware, Newark, DE 19716, USA

Abstract

We consider two classes of supersymmetric models with nonuniversal gaugino masses at M_{GUT} in an attempt to resolve the apparent muon $g-2$ anomaly encountered in the Standard Model. We explore two distinct scenarios, one in which all gaugino masses have the same sign at M_{GUT}, and a second case with opposite sign gaugino masses. The sfermion masses in both cases are assumed to be universal at M_{GUT}. We exploit the non universality among gaugino masses to realize large mass splitting between the colored and non-colored sfermions. Thus, the sleptons can have masses in the few hundred GeV range, whereas the colored sparticles turn out to be an order of magnitude or so heavier. In both models the resolution of the muon $g-2$ anomaly is compatible, among other things, with a $125-126$ GeV Higgs boson mass and the WMAP dark matter bounds.

---

[1]E-mail: ilia@bartol.udel.edu
   On leave of absence from: Andronikashvili Institute of Physics, Tbilisi, Georgia.
[2]E-mail: fariha@udel.edu
[3]E-mail: shafi@bartol.udel.edu
[4]E-mail: cemsalihun@bartol.udel.edu

1   Introduction

The ATLAS and CMS experiments at the Large Hadron Collider (LHC) have independently reported the discovery [1, 2] of a Standard Model (SM) like Higgs boson resonance of mass $m_h \simeq 125 - 126$ GeV using the combined 7 TeV and 8 TeV data. This discovery is compatible with low scale supersymmetry, since the Minimal Supersymmetric Standard Model (MSSM) predicts an upper bound of $m_h \lesssim 135$ GeV for the lightest CP-even Higgs boson [3].   Note that there exists a class of SO(10)-based supersymmetric models with third family Yukawa unification [4] in which the light CP even Higgs boson mass is predicted to be around 125 GeV [5]. On the other hand no signals for supersymmetric particles have shown up at the LHC and the current lower bounds on the colored sparticle masses, are

$$m_{\tilde{g}} \gtrsim 1.4 \text{ TeV (for } m_{\tilde{g}} \sim m_{\tilde{q}}) \quad \text{and} \quad m_{\tilde{g}} \gtrsim 0.9 \text{ TeV (for } m_{\tilde{g}} \ll m_{\tilde{q}}) \text{ [6, 7]).} \tag{1}$$

This has created some skepticism about the naturalness arguments employed for motivating low scale supersymmetry. Although the sparticle mass bounds in Eq. (1) are mostly derived for the R-parity conserving constrained MSSM (CMSSM), they are more or less applicable for a significant class of low scale supersymmetric models. In ref. [8] it was shown that there is room in the MSSM parameter space for the bounds in Eq. (1) to be relaxed, but it is not a large effect and the models are specific. The MSSM can accommodate $m_h \simeq 125$ GeV Higgs boson mass but it requires either a very large, $\mathcal{O}(\text{few} - 10)$ TeV, stop quark mass [9], or a large soft supersymmetry breaking (SSB) trilinear A_t-term, with a stop quark mass of around a TeV [10]. It is also interesting to note that a Higgs mass $m_h \simeq 125$ GeV also yields a lower bound on the top quark mass, $m_t \gtrsim 168$ GeV, independently from the values of the SSB parameters [11].

One of the most popular assumptions in low scale supersymmetric models is universal SSB mass terms (m_0) at M_{GUT} for the three generations of sfermions and masses $(M_{1/2})$ for the $SU(3)_c \times SU(2)_L \times U(1)_Y$ gauginos . The main motivation for assuming universal m_0 is based on the constraints obtained from flavor-changing neutral currents processes [12]. Moreover, the assumption of universal gaugino masses is inspired by the possible realization of a grand unified theory.   With a stop quark mass of more than 1 TeV (in order to achieve a 125 GeV light CP even Higgs boson), and with universal SSB parameters $M_{1/2}$ and m_0, the first and second generation squark masses lie in the multi-TeV range, and the corresponding smuon masses lie around the TeV scale.

On the other hand, the SM prediction for the anomalous magnetic moment of the muon [13], $a_\mu = (g - 2)_\mu/2$, shows a discrepancy with the experimental results [14],

which is quantified as follows:

$$\Delta a_\mu \equiv a_\mu(\text{exp}) - a_\mu(\text{SM}) = (28.6 \pm 8.0) \times 10^{-10} \qquad (2)$$

If supersymmetry is to resolve this discrepancy, one of the smuons and bino or wino SSB masses need to be quite light. Thus, it is hard to simultaneously explain the observed Higgs boson mass and resolve the muon $g-2$ anomaly with universal sfermion and gaugino SSB masses at M_{GUT}. A way out is to assume non universality in the gaugino sector at M_{GUT}. It is known that the gauginos provide different contributions to the squark and slepton renormalization group equations (RGEs) [12]. It is possible in this case to obtain colored sparticles with masses around a few TeV, while the slepton masses are around a few hundred GeV, if we assume that the gluino SSB mass term M_3 at M_{GUT} is a few times larger than the bino and wino SSB mass terms (M_1 and M_2). The parameters m_0, M_1 and M_2 can be in the few hundred GeV range.

To retain gauge coupling unification in the presence of nonuniversal gaugino masses at M_{GUT}, one could employ [15] non-singlet F-terms, compatible with the underlying GUT. Nonuniversal gauginos can also be generated from an F-term which is a linear combination of two distinct fields of different dimensions [16]. One can also consider two distinct sources for supersymmetry breaking [17]. With many distinct possibilities available for realizing nonuniversal gaugino masses while keeping universal sfermion mass at M_{GUT}, we employ three independent masses for the MSSM gauginos in our study. There have been several recent attempts to accommodate Δa_μ in Eq. (2) within the MSSM framework assuming specific models for nonuniversal SSB masses for gauginos [18]. In a recent paper [19], we explored the phenomenology of nonuniversal SSB gaugino masses and split sfermion families in the framework of third family Yukawa unification [4]. It was shown in [19] that the resolution of the muon $g-2$ anomaly is compatible, among other things, with the 125 GeV Higgs boson mass, the WMAP relic dark matter density and excellent t-b-τ Yukawa unification. In this paper we carry out a more thorough investigation of nonuniversal SSB gaugino masses and universal sfermion masses at M_{GUT} without insisting on Yukawa unification.

The outline of our paper is as follows. In section 2 we briefly describe the dominant contributions to the muon anomalous magnetic moment arising from low scale supersymmetry. In Section 3 we summarize the scanning procedure and the experimental constraints applied in our analysis. We also present the parameter space that we scan over. In Section 4 we assume nonuniversal gauginos at M_{GUT} with $M_3 < 0$, $M_2 > 0$ and $M_1 > 0$. Section 5 is dedicated to the case when same sign nonuniversal gaugino masses are assumed at M_{GUT}. The conclusion are presented in Section 6.

3

2   The Muon Anomalous Magnetic Moment

The leading contribution from low scale supersymmetry to the muon anomalous magnetic moment is given by [20, 21]:

$$
\begin{aligned}
\Delta a_\mu &= \frac{\alpha\, m_\mu^2\, \mu\, M_2 \tan\beta}{4\pi \sin^2\theta_W\, m_{\tilde{\mu}_L}^2} \left[\frac{f_\chi(M_2^2/m_{\tilde{\mu}_L}^2) - f_\chi(\mu^2/m_{\tilde{\mu}_L}^2)}{M_2^2 - \mu^2} \right] \\
&+ \frac{\alpha\, m_\mu^2\, \mu\, M_1 \tan\beta}{4\pi \cos^2\theta_W\, (m_{\tilde{\mu}_R}^2 - m_{\tilde{\mu}_L}^2)} \left[\frac{f_N(M_1^2/m_{\tilde{\mu}_R}^2)}{m_{\tilde{\mu}_R}^2} - \frac{f_N(M_1^2/m_{\tilde{\mu}_L}^2)}{m_{\tilde{\mu}_L}^2} \right] .
\end{aligned} \tag{3}
$$

Here α denotes the fine-structure constant, m_μ the muon mass, μ the bilinear Higgs mixing term and $\tan\beta$ is the ratio of the vacuum expectation values (VEVs) of the MSSM Higgs doublets. M_1 and M_2 denote the $U(1)_Y$ and $SU(2)$ gaugino masses respectively, θ_W is the weak mixing angle and $m_{\tilde{\mu}_L}$ ($m_{\tilde{\mu}_R}$) are left (right) handed smuon masses. The loop functions are defined as follows:

$$
f_\chi(x) = \frac{x^2 - 4x + 3 + 2\ln x}{(1-x)^3} , \qquad f_\chi(1) = -2/3, \tag{4}
$$

$$
f_N(x) = \frac{x^2 - 1 - 2x\ln x}{(1-x)^3} , \qquad f_N(1) = -1/3 . \tag{5}
$$

The first term in Eq. (3) stands for the dominant contribution coming from one loop diagram with Higgsinos, while the second term describes inputs from the bino-smuon loop. As the Higgsino mass μ increases, the first term decreases in Eq. (3) and the second term becomes dominant. The smuons, on the other hand, must be light, $\lesssim$ few hundred GeV, in both cases in order to provide sizeable contribution to the muon $g-2$ calculation. Note that the above formula will not be accurate for very large values of $\mu\tan\beta$, according to the decoupling theorem [20, 21]. From Eq. (3), the parameters

$$
M_1,\ M_2,\ \mu,\ \tan\beta, m_{\tilde{\mu}_L},\ m_{\tilde{\mu}_R}, \tag{6}
$$

are particularly relevant for the muon $g-2$ calculation, and we will quantify the desired parameter space later. Since we assume a universal the trilinear SSB term A_0, it follows that $A_\mu < \mu\tan\beta$ and we therefore do not consider the trilinear SSB-term contribution in Eq. 3.

3   Scanning Procedure and Experimental Constraints

We employ the ISAJET 7.84 package [22] to perform random scans over the parameter space. In this package, the weak scale values of gauge and third generation Yukawa

couplings are evolved to $M_{\rm GUT}$ via the MSSM RGEs in the $\overline{DR}$ regularization scheme. We do not strictly enforce the unification condition $g_3 = g_1 = g_2$ at $M_{\rm GUT}$, since a few percent deviation from unification can be assigned to unknown GUT-scale threshold corrections [23]. With the boundary conditions given at $M_{\rm GUT}$, all the SSB parameters, along with the gauge and third family Yukawa couplings, are evolved back to the weak scale $M_{\rm Z}$.

In evaluating the Yukawa couplings the SUSY threshold corrections [24] are taken into account at a common scale $M_S = \sqrt{m_{\tilde{t}_L} m_{\tilde{t}_R}}$. The entire parameter set is iteratively run between $M_{\rm Z}$ and $M_{\rm GUT}$ using the full 2-loop RGEs until a stable solution is obtained. To better account for the leading-log corrections, one-loop step-beta functions are adopted for the gauge and Yukawa couplings, and the SSB scalar mass parameters m_i are extracted from RGEs at appropriate scales $m_i = m_i(m_i)$. The RGE-improved 1-loop effective potential is minimized at an optimized scale M_S, which effectively accounts for the leading 2-loop corrections. Full 1-loop radiative corrections are incorporated for all sparticle masses.

In scanning the parameter space, we employ the Metropolis-Hastings algorithm as described in [25]. The data points collected all satisfy the requirement of radiative electroweak symmetry breaking (REWSB) [26], with the neutralino in each case being the LSP. After collecting the data, we impose the mass bounds on all the particles [27] and use the IsaTools package [28] to implement the various phenomenological constraints. We successively apply the following experimental constraints on the data that we acquire from ISAJET 7.84:

$$
\begin{array}{lll}
123 \text{ GeV} \leq m_h \leq 127 \text{ GeV} & [1, 2] \\
0.8 \times 10^{-9} \leq BR(B_s \rightarrow \mu^+ \mu^-) & \leq 6.2 \times 10^{-9} \ (2\sigma) & [29] \\
2.99 \times 10^{-4} \leq BR(b \rightarrow s\gamma) & \leq 3.87 \times 10^{-4} \ (2\sigma) & [30] \\
0.15 \leq \frac{BR(B_u \rightarrow \tau \nu_\tau)_{\rm MSSM}}{BR(B_u \rightarrow \tau \nu_\tau)_{\rm SM}} & \leq 2.41 \ (3\sigma) & [30] \\
0.0913 \leq \Omega_{\rm CDM} h^2 & \leq 0.1363 \ (5\sigma) & [32].
\end{array}
$$

We also implement the following mass bounds on the sparticle masses:

$$
\begin{array}{ll}
m_{\tilde{g}} \gtrsim 1.4 \text{ TeV (for } m_{\tilde{g}} \sim m_{\tilde{q}}) & [6, 7] \\
m_{\tilde{g}} \gtrsim 1 \text{ TeV (for } m_{\tilde{g}} \ll m_{\tilde{q}}) & [6, 7] \\
M_A \gtrsim 700 \text{ GeV (for } \tan\beta \simeq 48). & [31]
\end{array}
$$

Here $m_{\tilde{g}}$, $m_{\tilde{q}}$, M_A respectively stand for the gluino, first and second generation squarks and the CP odd Higgs boson masses.

4   Nonuniversal and opposite sign gaugino masses

In this section we discuss the scenario with nonuniversal and opposite sign gaugino masses at M_{GUT}, with the sfermion masses assumed to be universal. We will show that the muon $g-2$ anomaly can be explained in this model. We perform random scans for following ranges of the parameters:

$$0 \leq m_{16} \leq 3\,\mathrm{TeV}$$
$$0 \leq M_1 \leq 5\,\mathrm{TeV}$$
$$0 \leq M_2 \leq 5\,\mathrm{TeV}$$
$$-5 \leq M_3 \leq 0\,\mathrm{TeV}$$
$$-3 \leq A_0/m_{16} \leq 3$$
$$2 \leq \tan\beta \leq 60$$
$$0 \leq m_{10} \leq 5\,\mathrm{TeV}$$
$$\mu > 0. \tag{7}$$

Here m_{16} is the universal SSB mass parameter for sfermions, and M_1, M_2, and M_3 denote the SSB gaugino masses for $U(1)_Y$, $SU(2)_L$ and $SU(3)_c$ respectively. A_0 is the SSB trilinear scalar interaction coupling, $\tan\beta$ is the ratio of the MSSM Higgs vacuum expectation values (VEVs), and m_{10} is the SSB mass term for the MSSM Higgs doublets.

As previously mentioned in Section 2 (Eq. (6)), the quantities M_1, M_2, μ, $\tan\beta$, $m_{\tilde{\mu}_L}$, $m_{\tilde{\mu}_R}$, play an important role in the muon $g-2$ calculation. Based on this observation, in Figure 1 we present results in $\Delta a_\mu - m_{\tilde{\mu}_R}$, $\Delta a_\mu - m_{\tilde{\mu}_L}$, $\Delta a_\mu - m_{\tilde{\chi}_1^0}$, $\Delta a_\mu - \mu$, $\Delta a_\mu - \tan\beta$ and $\Delta a_\mu - m_{\tilde{W}^0}$ planes. *Gray* points are consistent with REWSB and neutralino LSP. *Yellow* points represent a subset for which Δa_μ lies within the 1σ interval in Eq. (2) . *Green* points form a subset of the *gray* ones and satisfy sparticles and Higgs mass bounds and all other constraints described in Section 3. *Brown* points belong to a subset of green points and satisfy the WMAP bound (5σ) on neutralino dark matter abundance.

Overall, from Figure 1 we learn that in order to provide the desired SUSY contributions to Δa_μ , while staying consistent with all the experimental constraints described in Section 3, we should impose the following: 200 GeV $\lesssim m_{\tilde{\mu}_R} \lesssim$ 700 GeV, 400 GeV $\lesssim m_{\tilde{\mu}_L} \lesssim$ 800 GeV, 100 GeV $\lesssim m_{\tilde{\chi}_1^0} \lesssim$ 400 GeV, 9 $\lesssim \tan\beta \lesssim$ 44, 100 GeV $\lesssim m_{\tilde{W}^0} \lesssim$ 1.1 TeV.

The salient features of the results in Figure 1 can be understood by referring to Eq. (3). We have two dominant contributions at one loop level arising from sparticles
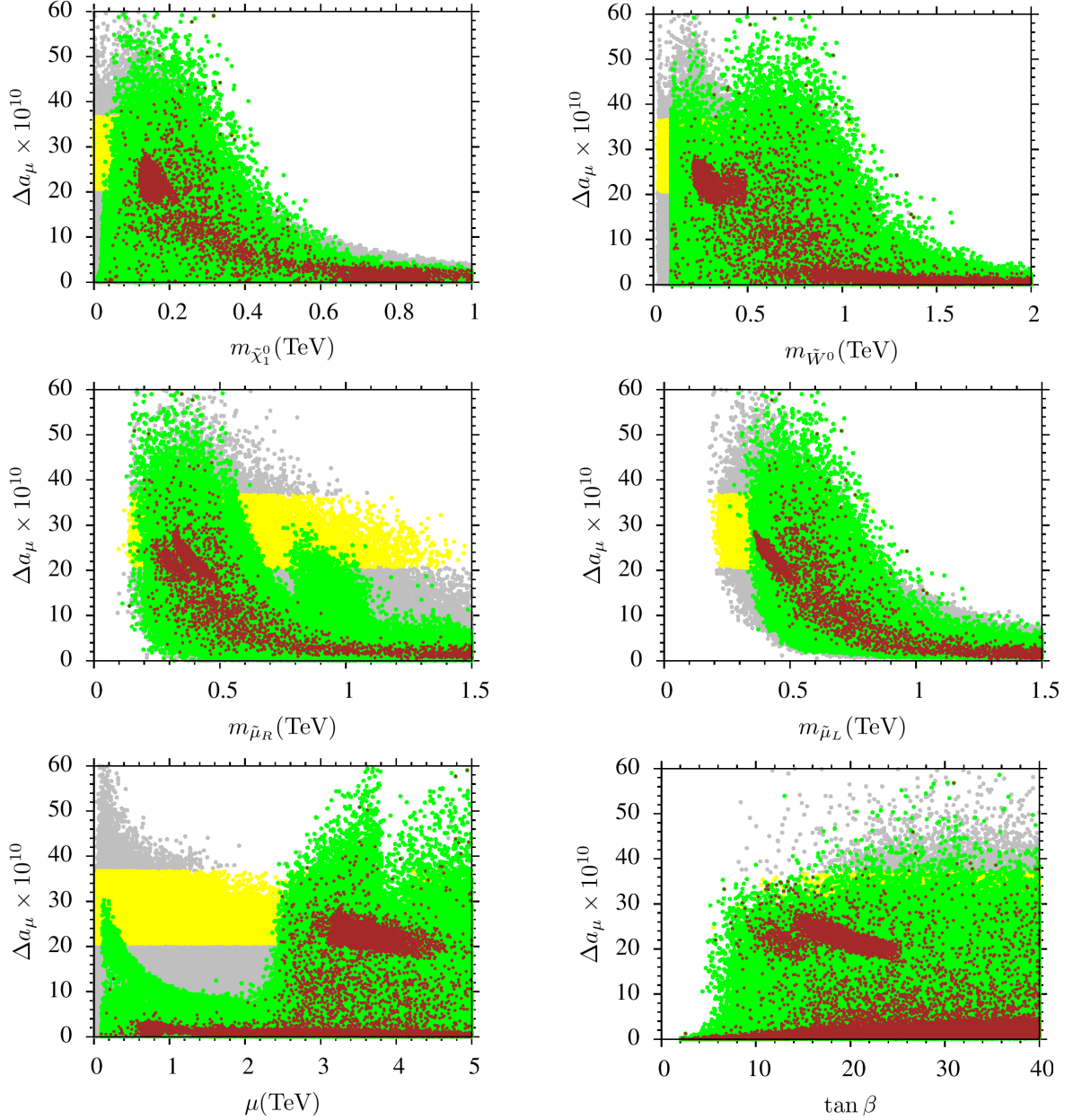
6

Figure 1: Plots in the $\Delta a_\mu - m_{\tilde{\mu}_R}$, $\Delta a_\mu - m_{\tilde{\mu}_L}$, $\Delta a_\mu - m_{\tilde{\chi}_1^0}$, $\Delta a_\mu - m_{\tilde{W}^0}$, $\Delta a_\mu - \mu$ and $\Delta a_\mu - \tan\beta$ planes. *Gray* points are consistent with REWSB and neutralino LSP. *Yellow* points have Δa_μ in the 1σ interval in Eq. (2). *Green* points form a subset of the *gray* ones and satisfy sparticles and Higgs mass bounds and all other constraints described in Section 3. *Brown* points belong to a subset of green points and satisfy the WMAP bound (5σ) on neutralino dark matter abundance.

7

in the loop. The first term in Eq. (3) stands for contributions involving Higgsinos, while the second term describes the bino-smuon contribution. As the Higgs bilinear μ term increases, the contribution from the loop involving the Higgsinos decreases, while the bino-smuon loop becomes more relevant. This is the reason why in the spectrum we can have relatively heavy wino, $O(TeV)$, and still maintain sufficient contribution to muon $g-2$. Since in our setup the gauginos are arbitrary at M_{GUT} and m_0 is $O(\text{few hundred})$ GeV or so, we can have a large difference between the left and right handed smuon masses from RGE running. This allows one to provide a significant contribution to muon $g-2$ from the loop involving either the left or right handed smuons. Thus, we can have one of them around a TeV, while the lighter one is $O(\text{few hundred})$ GeV. Since in our study μ values up to 5 TeV are allowed, the parameter $\tan\beta$ can lie in the fairly wide interval $9 \lesssim \tan\beta \lesssim 44$.

The impact of the muon $g-2$ anomaly on the fundamental parameters is presented in Figure 2, which shows the results in the $\Delta a_\mu - M_3/M_1$, $\Delta a_\mu - M_3/M_2$, $\Delta a_\mu - M_2/M_1$, $\Delta a_\mu - M_2$, $\Delta a_\mu - M_3$ and $\Delta a_\mu - m_{16}$ planes, with the color coding the same as in Figure 1. From these results we find the requirements, $|M_3/M_1| \leq 0.8$ and $|M_3/M_2| \leq 2.4$. The latter ratio is almost the inverse of what was obtained in resolving the little hierarchy problem in the MSSM [33]. There is no preferred range for the ratio M_2/M_1, since diagrams involving only M_2 or M_1 can provide sufficient contribution to muon $g-2$ [20, 21].

The $\Delta a_\mu - M_2$ plane shows that $M_2 \lesssim 1.3$ TeV at M_{GUT}, in contrast to M_3 for which $|M_3| \gtrsim 2$ TeV. The last ($\Delta a_\mu - m_{16}$) panel, in Figure 2 shows that m_{16} cannot be heavier than ~ 700 GeV if we require a significant contribution to muon $g-2$.

The $m_{\tilde{\mu}_R} - m_{\tilde{\chi}_1^0}$, $m_{\tilde{\tau}_1} - m_{\tilde{\chi}_1^0}$, $m_{\tilde{\chi}_1^\pm} - m_{\tilde{\chi}_1^0}$ and $m_A - m_{\tilde{\chi}_1^0}$ panels of Figure 3 show that there are a variety of channels that reduce the relic abundance of neutralino LSP to the desired range applied for the dark matter relic density. All points are consistent with REWSB and neutralino LSP. Green points satisfy all mass bounds and B-physics constraints. Yellow points form a subset of green and they indicate solutions with the desired contribution to muon $g-2$. Brown points are a subset of yellow and satisfy the WMAP bound (5σ) on neutralino dark matter abundance. Since muon $g-2$ requires light smuons, it is perhaps not surprising to realize the smuon-neutralino coannihilation scenario, as seen in the $m_{\tilde{\mu}_R} - m_{\tilde{\chi}_1^0}$ plane. Moreover, in the case of universal sfermion families this also constrains the third family sfermions to be light. The lightest stau mass lies in the range $\sim 100-450$ GeV, and the $m_{\tilde{\tau}_1} - m_{\tilde{\chi}_1^0}$ plane shows the stau-neutralino coannihilation solutions. Similarly the $m_{\tilde{\chi}_1^\pm} - m_{\tilde{\chi}_1^0}$ and $m_A - m_{\tilde{\chi}_1^0}$ panels display the chargino-neutralino coannihilation and A-resonance scenarios respectively.

We display the results for the squarks and gluino spectra in the $m_{\tilde{q}}$-$m_{\tilde{g}}$ plane in
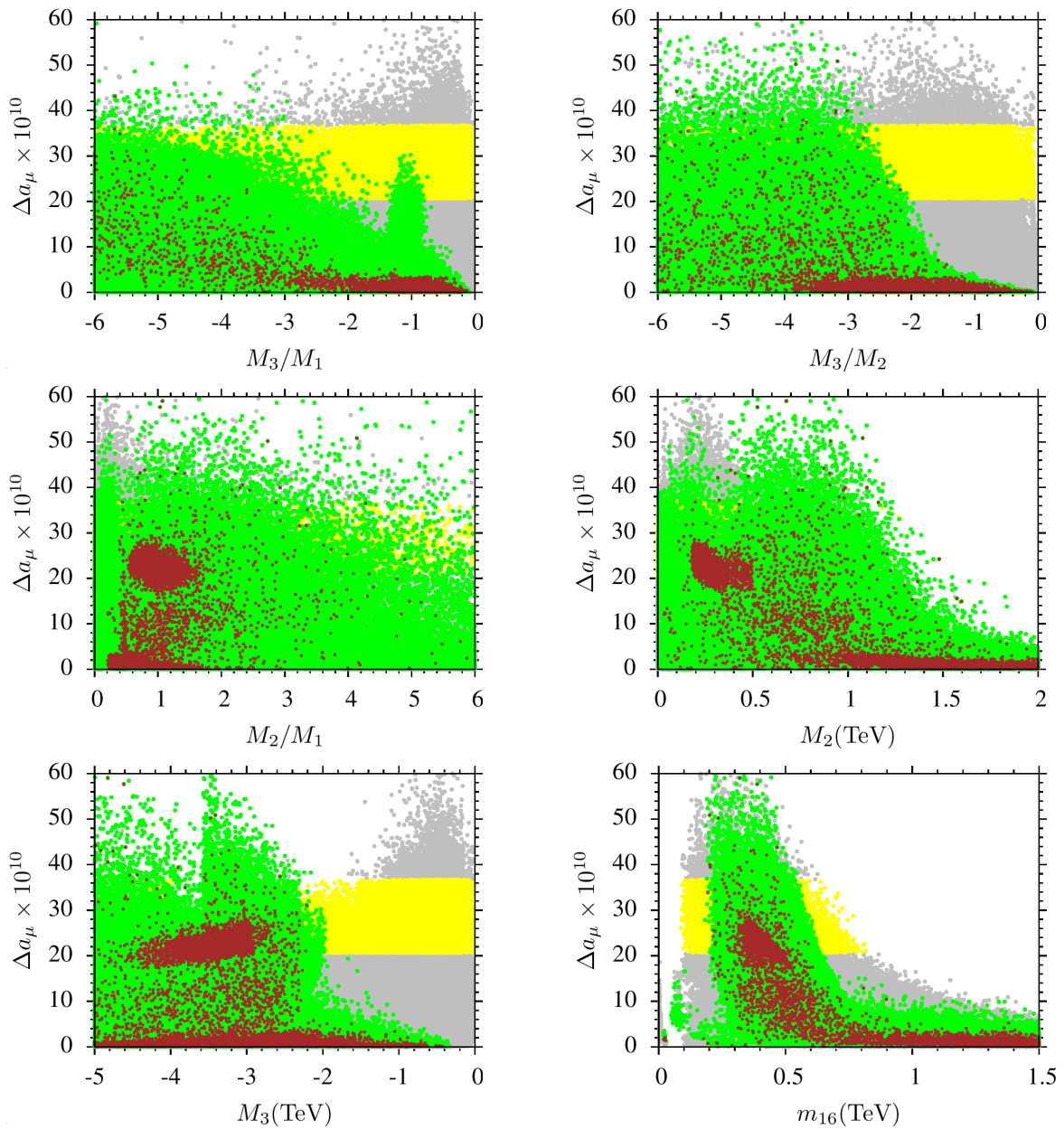
8

Figure 2: Plots in the $\Delta a_\mu - M_3/M_1$, $\Delta a_\mu - M_3/M_2$, $\Delta a_\mu - M_2/M_1$, $\Delta a_\mu - M_2$, $\Delta a_\mu - M_3$ and $\Delta a_\mu - m_{16}$ planes. Color coding is the same as in Figure 1.
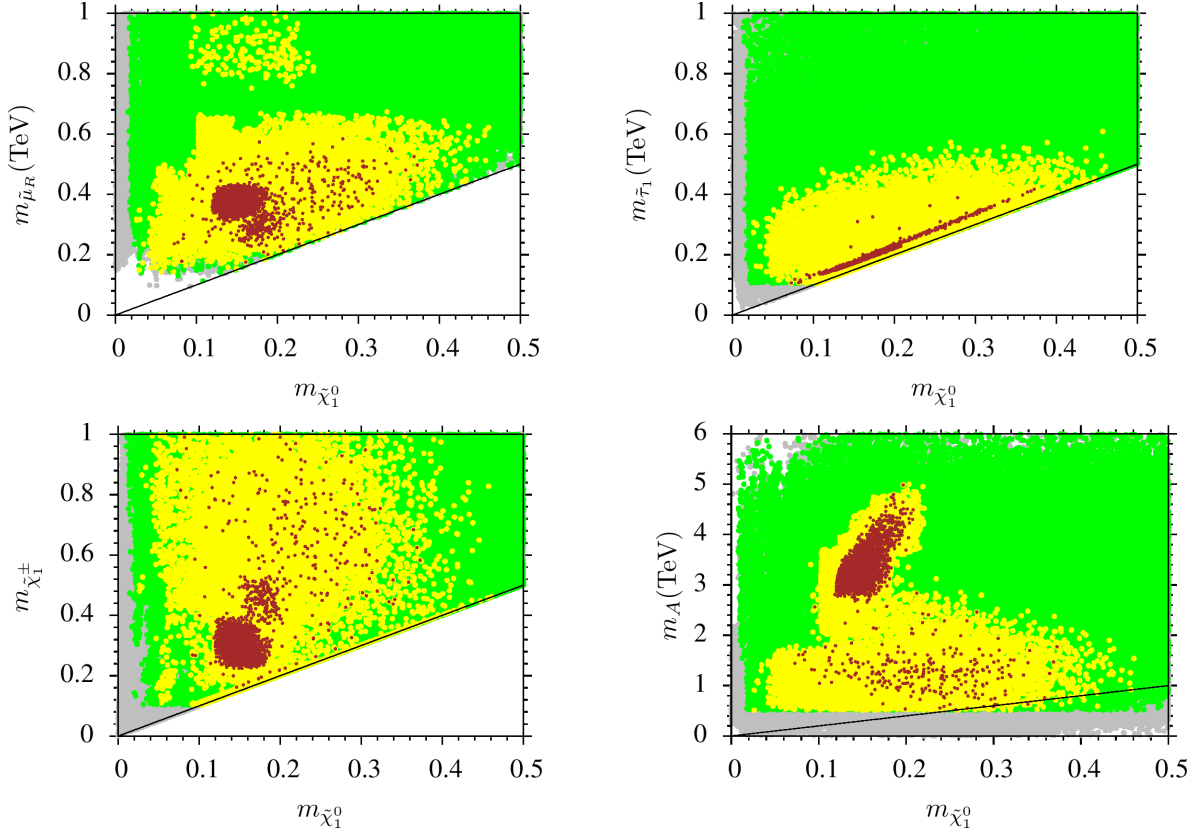
Figure 3: Plots in the $m_{\tilde{\mu}_R} - m_{\tilde{\chi}_1^0}$, $m_{\tilde{\tau}_1} - m_{\tilde{\chi}_1^0}$, $m_{\tilde{\chi}_1^\pm} - m_{\tilde{\chi}_1^0}$ and $m_A - m_{\tilde{\chi}_1^0}$ planes. All points are consistent with REWSB and neutralino LSP. Green points satisfy mass bounds and B-physics constraints. Yellow points form a subset of green and they indicate solutions with muon $g - 2$ within 1σ deviation from its theoretical value. Brown points are a subset of yellow and satisfy the WMAP bound (5σ) on neutralino dark matter abundance.
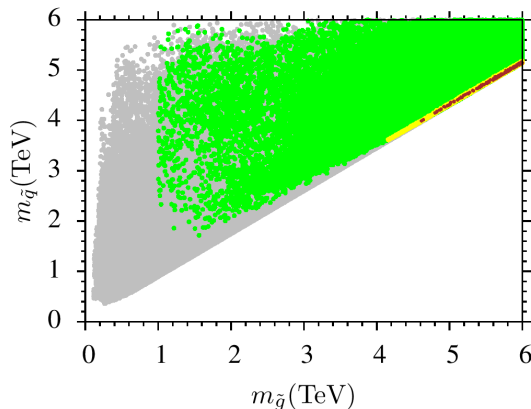
Figure 4: Plot in the $m_{\tilde{q}}$-$m_{\tilde{g}}$ plane. Color coding is the same as in Figure 3.

Figure 4, with the color coding the same as in Figure 3. In this scenario muon $g - 2$ allows solutions with $m_{\tilde{q}}, m_{\tilde{g}} \gtrsim 4$ TeV. Heavy gluino masses are explained with large values of M_3 at M_{GUT} as shown in Figure 2, which also lifts up the squark masses with the resultant heavy spectrum for squarks, even though the squarks and sleptons have the universal mass at M_{GUT}.

Table 1 lists four benchmark points that satisfy the constraints described in Section 3 and yield the desired Δa_{μ}. For points 1-4, the LSP neutralino relic density satisfies the WMAP bound, realized via smuon-neutralino, stau-neutralino and chargino-neutralino coannihilation channels and the A-resonance solution, respectively. The gluino is the heaviest colored sparticle for the four benchmark points.

5 Nonuniversal and same sign gaugino masses

In this section we discuss the scenario with nonuniversal and same sign gaugino masses, but with universal sfermion mass at M_{GUT}. The parameter space scanned in

	Point 1	Point 2	Point 3	Point 4
m_{16}	302.9	513.6	528	422.9
M_1	357	428.2	554.4	618.2
M_2	498.8	497.6	255.6	567.1
M_3	-4061	-4769	-3027	-3490
$\tan\beta$	9.3	39.2	42.7	43.3
A_0/m_{16}	-0.36	0.84	-0.71	-0.72
m_{10}	716.2	806.6	588.2	158.8
m_t	173.3	173.3	173.3	173.3
Δa_μ	$\mathbf{24.0 \times 10^{-10}}$	$\mathbf{28.9 \times 10^{-10}}$	$\mathbf{21.4 \times 10^{-10}}$	$\mathbf{27.2 \times 10^{-10}}$
m_h	**122.4**	**124.5**	**123.0**	**123.7**
m_H	4278	2422	1082	626.4
m_A	4250	2406	1075	**622.3**
$m_{H^\pm}$	4279	2424	1087	634.4
$m_{\tilde\chi^0_{1,2}}$	**188.2**,516	**225.4**, 528.4	**268**, **287.7**	**301.6**, 563.3
$m_{\tilde\chi^0_{3,4}}$	41276, 4127	4806, 4806	3155, 3155	3600, 3600
$m_{\tilde\chi^\pm_{1,2}}$	520.1, 4089	530.4, 4761	**289**, 3126	565.3, 3567
$m_{\tilde g}$	8137	9471	6198	7063
$m_{\tilde u_{L,R}}$	6929, 6947	8064, 8088	5329, 5348	6050, 6059
$m_{\tilde t_{1,2}}$	6004, 6534	6998, 7184	4617, 4738	5244, 5360
$m_{\tilde d_{L,R}}$	6929, 6952	8065, 8088	5329, 5350	6051, 6062
$m_{\tilde b_{1,2}}$	6494, 6912	7122, 7278	4642, 4764	5234, 5364
$m_{\tilde\nu_{1,2}}$	267.6	491	509.5	516.9
$m_{\tilde\nu_3}$	291.9	665.3	583.2	667.9
$m_{\tilde e_{L,R}}$	437.1, **201.2**	531.1, 502	521.9, 556.8	526.5, 464.1
$m_{\tilde\tau_{1,2}}$	**207.9**, 418.6	**262.6**, 840.1	302.8, 743.6	342.5, 813.4
σ_{SI}(pb)	0.26×10^{-12}	0.56×10^{-14}	0.34×10^{-11}	0.17×10^{-10}
σ_{SD}(pb)	0.17×10^{-9}	0.93×10^{-10}	0.70×10^{-9}	0.32×10^{-9}
$\Omega_{CDM}h^2$	0.11	0.11	0.10	0.11

Table 1: Masses in this table are in GeV units. All points yield Δa_μ in Eq. (2) within 1σ, and satisfy the sparticle mass and B-physics constraints described in Section 3. Points 1-4 respectively correspond to smuon-neutralino, stau-neutralino, chargino-neutralino coannihilation channels and A-resonance solutions for neutralino dark mater candidate.

this case is as follows:

$$0 \leq m_{16} \leq 3\,\text{TeV}$$
$$0 \leq M_1 \leq 5\,\text{TeV}$$
$$0 \leq M_2 \leq 5\,\text{TeV}$$
$$0 \leq M_3 \leq 5\,\text{TeV}$$
$$-3 \leq A_0/m_{16} \leq 3$$
$$2 \leq tan\beta \leq 60$$
$$0 \leq m_{10} \leq 5\,\text{TeV}$$
$$\mu > 0 \tag{8}$$

Figure 5 shows the results in the $\Delta a_\mu - m_{\tilde{\mu}_R}$, $\Delta a_\mu - m_{\tilde{\mu}_L}$, $\Delta a_\mu - m_{\tilde{\chi}_1^0}$, $\Delta a_\mu - \mu$, $\Delta a_\mu - \tan\beta$ and $\Delta a_\mu - m_{\tilde{W}^0}$ planes and the color coding is the same as in Figure 1. The results are similar to what we had in the previous section. The small difference arises because of the opposite sign of the gaugino masses, especially when the gluino mass is large compared to the other SSB mass parameters. In this case, the RGE running and supersymmetric thresholds provide different contributions to the RGEs of the stop quark masses and A_t [24, 34, 35]. On the other hand, these two quantities provide the dominant contribution to the radiative correction to the mass of the mass of the light CP even Higgs. We find that the reduction of green points in Figure 5 compared to Figure 1 occurs because of the Higgs boson mass bound, $122\,\text{GeV} \leq m_h \leq 127\,\text{GeV}$.

The figure in $\Delta a_\mu - m_{\tilde{\mu}_R}$ plane shows that the right-handed smuon can be as heavy as 1 TeV or so, while the left-handed smuon is bounded in a region of order $350 - 700\,\text{GeV}$ as seen in the $\Delta a_\mu - m_{\tilde{\mu}_L}$ plane. We can see from the $\Delta a_\mu - m_{\tilde{\chi}_1^0}$ plane that only solutions with a light LSP ($\sim 100 - 300\,\text{GeV}$) are allowed by the muon $g - 2$ constraint. The $\Delta a_\mu - \mu$ plane indicates that a sizable contribution to muon $g - 2$ prefers mostly large values of μ, but smaller values are also possible as discussed in the previous section. It is possible to find solutions with a wide range of $\tan\beta$, even though the contributions to $g - 2$ slightly decrease as $\tan\beta$ increases. Also, the wino cannot be heavier than $\sim 700\,\text{GeV}$ in order to have significant contributions to muon $g - 2$.

Figure 6 shows the gaugino mass ratios, and the gaugino and sfermion masses at M_{GUT} in the $\Delta a_\mu - M_3/M_1$, $\Delta a_\mu - M_3/M_2$, $\Delta a_\mu - M_2/M_1$, $\Delta a_\mu - M_2$, $\Delta a_\mu - M_3$ and $\Delta a_\mu - m_{16}$ planes, with the color coding as in Figure 1. We find $|M_3|/|M_1| \gtrsim 1$, while $|M_3|/|M_2| \gtrsim 3.4$. In contrast to the previous case, the 1σ limit on $g - 2$ requires the ratio $|M_2|/|M_1| \lesssim 2.5$. As seen from the $\Delta a_\mu - M_2$ panel, muon $g - 2$ prefers $M_2 \lesssim 1$ TeV, while it allows only large values of M_3 ($\gtrsim 2$ TeV) dictated by the 125 GeV
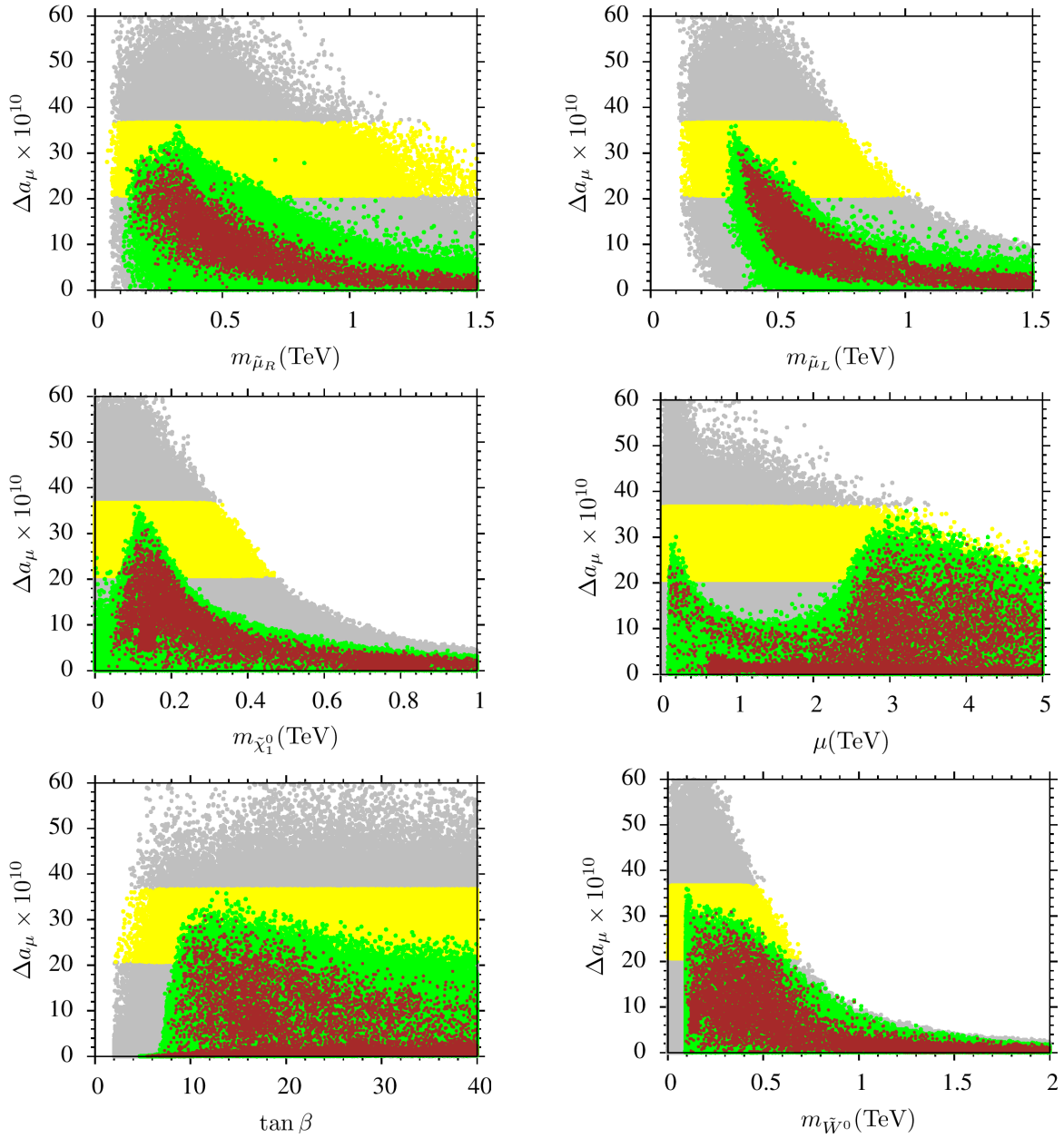
13

Figure 5: Plots in the $\Delta a_\mu - m_{\tilde{\mu}_R}$, $\Delta a_\mu - m_{\tilde{\mu}_L}$, $\Delta a_\mu - m_{\tilde{\chi}_1^0}$, $\Delta a_\mu - \mu$, $\Delta a_\mu - \tan\beta$ and $\Delta a_\mu - m_{\tilde{W}^0}$ planes. Color coding is the same as in Figure 1.
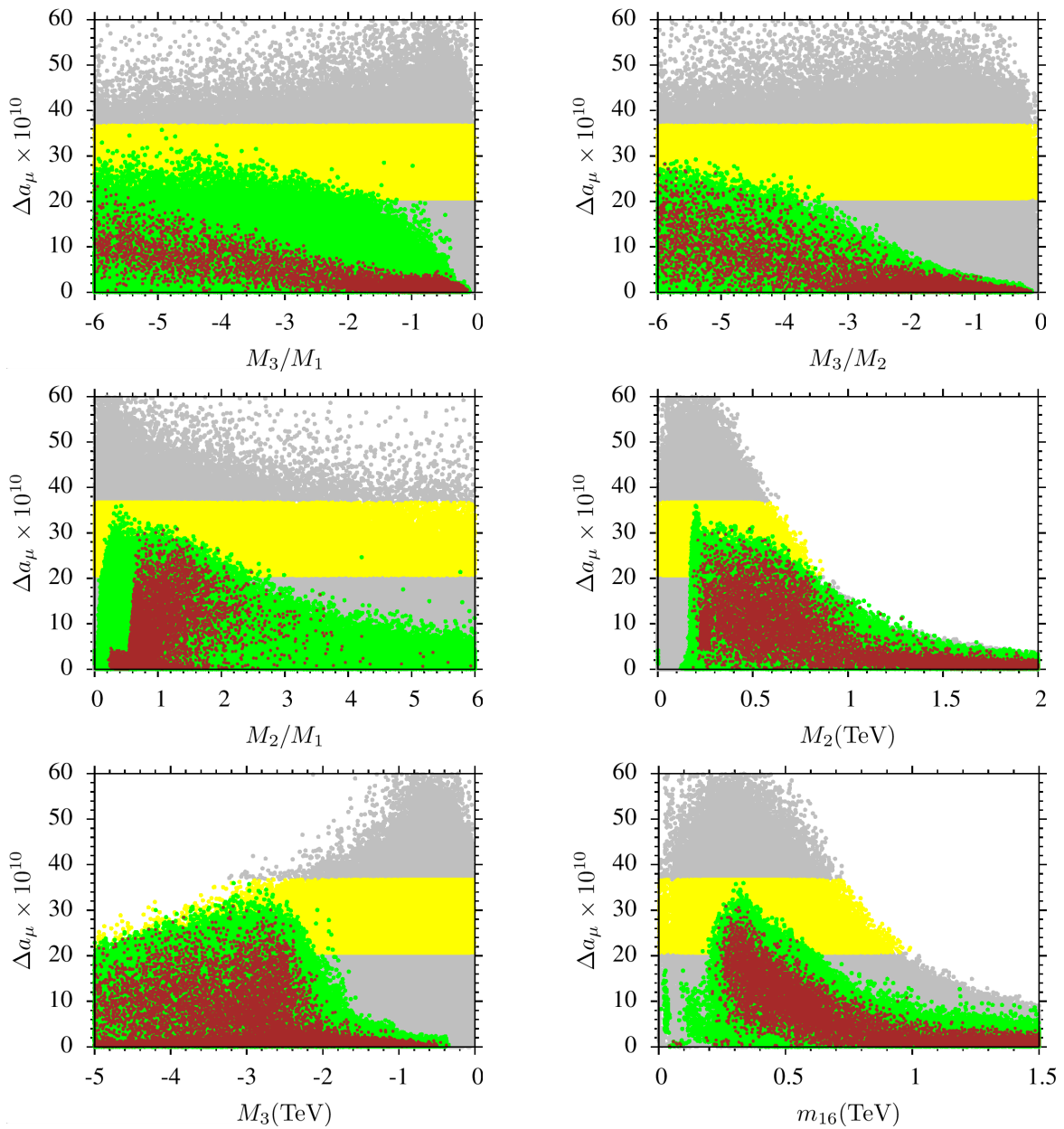
Figure 6: plots in $\Delta a_\mu - M_3/M_1$, $\Delta a_\mu - M_3/M_2$, $\Delta a_\mu - M_2/M_1$, $\Delta a_\mu - M_2$, $\Delta a_\mu - M_3$ and $\Delta a_\mu - m_{16}$ planes. Color coding is the same as in Figure 1.
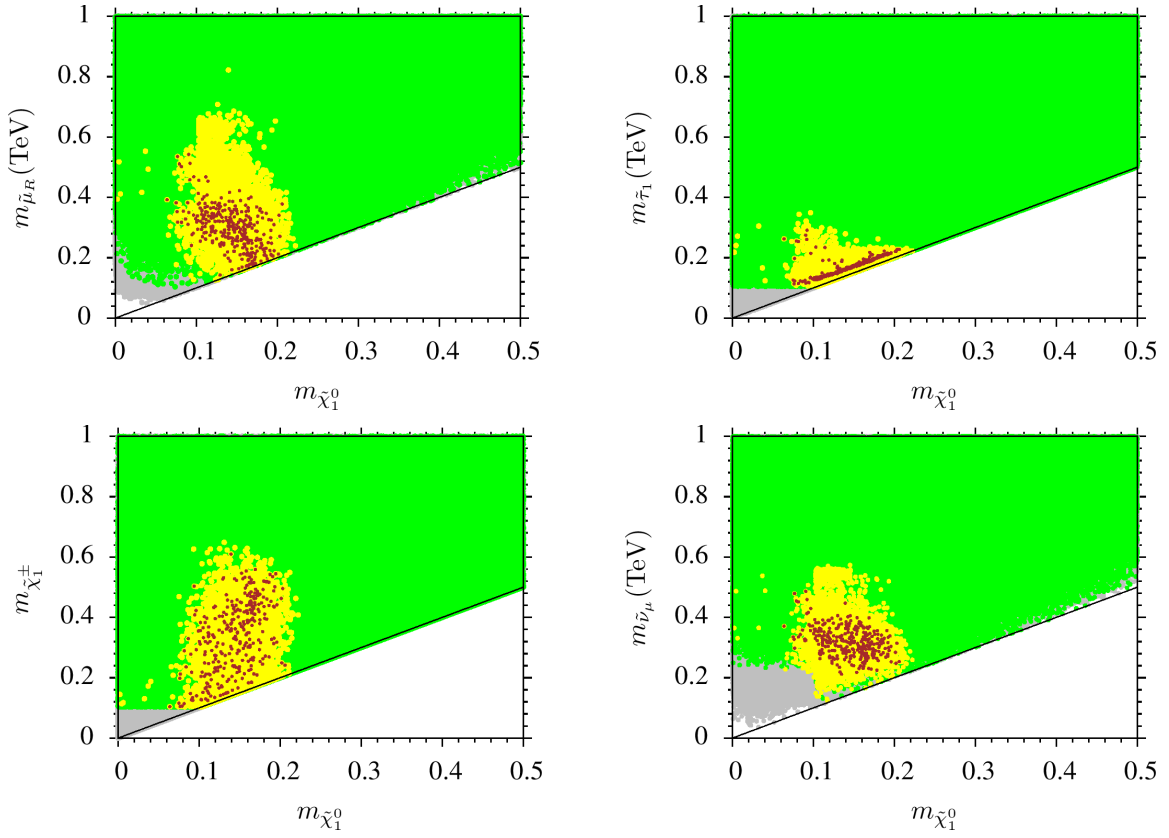
Figure 7: Plots in the $m_{\tilde{\mu}_R} - m_{\tilde{\chi}_1^0}$, $m_{\tilde{\tau}_1} - m_{\tilde{\chi}_1^0}$, $m_{\tilde{\chi}_1^\pm} - m_{\tilde{\chi}_1^0}$ and $m_{\tilde{\nu}_\mu} - m_{\tilde{\chi}_1^0}$ planes. Color coding is the same as in Figure 3.
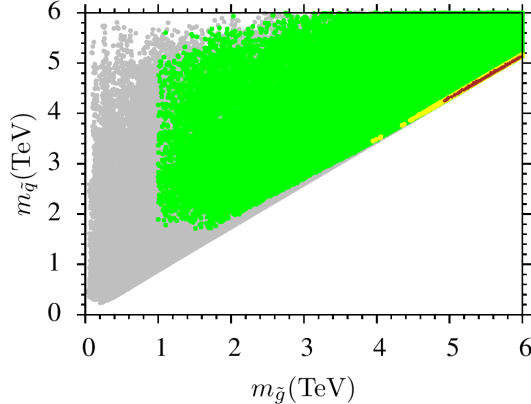
16

Figure 8: Plot in the $m_{\tilde{q}}$-$m_{\tilde{g}}$ plane. Color coding is the same as in Figure 3.

Higgs boson requirement. As expected, the sfermion masses turn out to be light, and the $\Delta a_\mu - m_{16}$ plane shows that the m_{16} can be as heavy as ~ 700 GeV.

Figure 7 displays the possible coannihilation channels in the $m_{\tilde{\mu}_R} - m_{\tilde{\chi}_1^0}$, $m_{\tilde{\tau}_1} - m_{\tilde{\chi}_1^0}$, $m_{\tilde{\chi}_1^\pm} - m_{\tilde{\chi}_1^0}$ and $m_{\tilde{\nu}_\mu} - m_{\tilde{\chi}_1^0}$ panels. Since this scenario allows only light LSP solutions, the coannihilation channels require the appropriate NLSP to be sufficiently light and nearly degenerate with the LSP. The coannihilation scenarios are similar to those in the previous section. On the other hand, there is no solution corresponding to the A-resonance, while sneutrino-neutralino coannihilation channel is possible in this scenario. Figure 8 shows the result for the squarks and gluino spectra, and we find a heavy spectrum for the colored sparticles ($m_{\tilde{q}} \gtrsim 3$ TeV and $m_{\tilde{g}} \gtrsim 4$ TeV), similar to the scenario in the previous section.

Table 2 lists three benchmark points for this scenario that satisfy all the constraints described in Section 3. The colored sparticles are all quite heavy while the sleptons are light ($\sim$ few hundred GeV). Points 1-3 respectively correspond to smuon-neutralino, stau-neutralino and chargino-neutralino coannihilation channels.

6   Conclusion

We have explored two classes of supersymmetric models with nonuniversal gaugino masses at M_{GUT} in order to resolve the muon $g - 2$ anomaly encountered in the Standard Model. In both models we find that the resolution of this anomaly is compatible with the presence of a SM-like Higgs boson of mass 125-126 GeV, and the relic LSP neutralino density is compatible with the WMAP dark matter bounds.

17

	Point 1	Point 2	Point 3
m_{16}	309.2	456.2	382.3
M_1	497.7	427.6	425.7
M_2	720.5	442.1	276.4
M_3	4610	4724	3030
$\tan\beta$	10.5	16.1	15.4
A_0/m_{16}	-0.16	-0.03	2.37
m_{10}	1280	241.5	391.1
m_t	173.3	173.3	173.3
Δa_μ	$\mathbf{20.7 \times 10^{-10}}$	$\mathbf{22.6 \times 10^{-10}}$	$\mathbf{21.1 \times 10^{-10}}$
m_h	**123.1**	**123.8**	**122.1**
m_H	4868	4823	3165
m_A	4837	4792	3145
$m_{H^\pm}$	4869	4824	3166
$m_{\tilde{\chi}^0_{1,2}}$	**187.4**, 537.4	**154.5**, 295.2	**161.6**, **175.9**
$m_{\tilde{\chi}^0_{3,4}}$	4600, 4600	4819, 4819	3135, 3135
$m_{\tilde{\chi}^\pm_{1,2}}$	541.8, 4558	297.4, 4775	**177.5**, 3107
$m_{\tilde{g}}$	9153	9399	6206
$m_{\tilde{u}_{L,R}}$	7784, 7806	7997, 8021	5320, 5337
$m_{\tilde{t}_{1,2}}$	6693, 7316	6927, 7518	4630, 5019
$m_{\tilde{d}_{L,R}}$	7784, 7806	7997, 8027	5321, 5341
$m_{\tilde{b}_{1,2}}$	7279, 7764	7480, 7955	4987, 5296
$m_{\tilde{\nu}_{1,2}}$	330.5	291.7	302.7
$m_{\tilde{\nu}_3}$	354.2	342.6	313.6
$m_{\tilde{e}_{L,R}}$	510.3, **196**	487, 389.5	392.3, 372.4
$m_{\tilde{\tau}_{1,2}}$	221.4, 470.1	**180.3**, 544.3	212.1, 456.8
σ_{SI}(pb)	0.95×10^{-13}	0.26×10^{-15}	0.21×10^{-12}
σ_{SD}(pb)	0.11×10^{-9}	0.88×10^{-10}	0.59×10^{-9}
$\Omega_{CDM}h^2$	0.11	0.12	0.09

Table 2: Masses in this table are in GeV units. All points yield Δa_μ in Eq. (2) within 1σ, and satisfy the sparticle mass and B-physics constraints described in Section 3.. Points 1-3 respectively correspond to smuon-neutralino, stau-neutralino, chargino-neutralino coannihilation channels.

The Higgs mass bound requires that the colored sparticles are quite heavy, $\gtrsim 3$ TeV, but the sleptons including the smuons can be an order of magnitude or so lighter ($\gtrsim 200$ GeV.)

Acknowledgments

References

[1] G. Aad *et al.* [ATLAS Collaboration], Phys. Lett. B **716**, 1 (2012).

[2] S. Chatrchyan *et al.* [CMS Collaboration], Phys. Lett. B **716**, 30 (2012).

[3] M. S. Carena and H. E. Haber, Prog. Part. Nucl. Phys. **50**, 63 (2003) and references therein.

[4] B. Ananthanarayan, G. Lazarides and Q. Shafi, Phys. Rev. D **44**, 1613 (1991; Phys. Lett. B **300**, 24 (1993)5; Q. Shafi and B. Ananthanarayan, Trieste HEP Cosmol.1991:233-244.

[5] I. Gogoladze, Q. Shafi and C. S. Un, JHEP **1208**, 028 (2012); M. Adeel Ajaib, I. Gogoladze, Q. Shafi and C. S. Un, JHEP **1307**, 139 (2013).

[6] G. Aad *et al.* [ATLAS Collaboration], Phys. Rev. D **87**, 012008 (2013).

[7] S. Chatrchyan *et al.* [CMS Collaboration], JHEP **1210**, 018 (2012).

[8] B. Bhattacherjee, J. L. Evans, M. Ibe, S. Matsumoto and T. T. Yanagida, arXiv:1301.2336 [hep-ph].

[9] M. A. Ajaib, I. Gogoladze, F. Nasir and Q. Shafi, Phys. Lett. B **713**, 462 (2012).

[10] For a review see A. Djouadi, Phys. Rept. **459**, 1 (2008) and reference therein.

[11] I. Gogoladze, R. Khalid, S. Raza and Q. Shafi, arXiv:1402.2924 [hep-ph].

[12] See, for instance, S. P. Martin, arXiv:hep-ph/9709356 [hep-ph] and references therein.

[13] M. Davier, A. Hoecker, B. Malaescu and Z. Zhang, Eur. Phys. J. C **71**, 1515 (2011) [Erratum-ibid. C **72**, 1874 (2012)]; K. Hagiwara, R. Liao, A. D. Martin, D. Nomura and T. Teubner, J. Phys. G **38**, 085003 (2011).

[14] G. W. Bennett *et al.* [Muon G-2 Collaboration], Phys. Rev. D **73**, 072003 (2006); G. W. Bennett *et al.* [Muon (g-2) Collaboration], Phys. Rev. D **80**, 052008 (2009)

[15] B. Ananthanarayan, P. N. Pandita, Int. J. Mod. Phys. **A22**, 3229-3259 (2007); S. Bhattacharya, A. Datta and B. Mukhopadhyaya, JHEP **0710**, 080 (2007); S. P. Martin, Phys. Rev. **D79**, 095019 (2009); J. Chakrabortty and A. Raychaudhuri, Phys. Lett. B **673**, 57 (2009).

[16] S. P. Martin, arXiv:1312.0582 [hep-ph].

[17] A. Anandakrishnan and S. Raby, Phys. Rev. Lett. **111**, 211801 (2013).

[18] M. Endo, K. Hamaguchi, S. Iwamoto and T. Yoshinaga, JHEP **1401**, 123 (2014); S. Mohanty, S. Rao and D. P. Roy, JHEP **1309**, 027 (2013); S. Akula and P. Nath, Phys. Rev. D **87**, 115022 (2013); M. Endo, K. Hamaguchi, T. Kitahara and T. Yoshinaga, JHEP **1311**, 013 (2013); J. Chakrabortty, S. Mohanty and S. Rao, arXiv:1310.3620 [hep-ph].

[19] M. A. Ajaib, I. Gogoladze, Q. Shafi and C. S. Un, arXiv:1402.4918 [hep-ph].

[20] T. Moroi, Phys. Rev. D **53**, 6565 (1996) [Erratum-ibid. D **56**, 4424 (1997)];

[21] S. P. Martin and J. D. Wells, Phys. Rev. D **64**, 035003 (2001). G. F. Giudice, P. Paradisi, A. Strumia and A. Strumia, JHEP **1210**, 186 (2012)

[22] F. E. Paige, S. D. Protopopescu, H. Baer and X. Tata, hep-ph/0312045.

[23] J. Hisano, H. Murayama , and T. Yanagida, Nucl. Phys. **B402** (1993) 46. Y. Yamada, Z. Phys. **C60** (1993) 83; J. L. Chkareuli and I. G. Gogoladze, Phys. Rev. D **58**, 055011 (1998).

[24] D. M. Pierce, J. A. Bagger, K. T. Matchev, and R.-j. Zhang, Nucl. Phys. **B491** (1997) 3.

[25] G. Belanger, F. Boudjema, A. Pukhov and R. K. Singh, JHEP **0911**, 026 (2009); H. Baer, S. Kraml, S. Sekmen and H. Summy, JHEP **0803**, 056 (2008).

[26] L. E. Ibanez and G. G. Ross, Phys. Lett. **B110** (1982) 215; K. Inoue, A. Kakuto, H. Komatsu and S. Takeshita, Prog. Theor. Phys. **68**, 927 (1982) [Erratum-ibid. **70**, 330 (1983)]; L. E. Ibanez, Phys. Lett. **B118** (1982) 73; J. R. Ellis, D. V. Nanopoulos, and K. Tamvakis, Phys. Lett. **B121** (1983) 123; L. Alvarez-Gaume, J. Polchinski, and M. B. Wise, Nucl. Phys. **B221** (1983) 495.

[27] J. Beringer *et al.* [Particle Data Group Collaboration], Phys. Rev. D **86**, 010001 (2012).

[28] H. Baer, C. Balazs, and A. Belyaev, JHEP **03** (2002) 042; H. Baer, C. Balazs, J. Ferrandis, and X. Tata Phys. Rev. **D64** (2001) 035004.

[29] T. Aaltonen *et al.* [CDF Collaboration], Phys. Rev. Lett. **100**, 101802 (2008).

[30] E. Barberio *et al.* [Heavy Flavor Averaging Group], arXiv:0808.1297 [hep-ex].

[31] The CMS Collaboration, CMS-PAS-HIG-12-050.

[32] G. Hinshaw *et al.* [WMAP Collaboration], arXiv:1212.5226 [astro-ph.CO].

[33] I. Gogoladze, F. .Nasir and Q. .Shafi, Int. J. Mod. Phys. A **28**, 1350046 (2013); I. Gogoladze, F. Nasir and Q. Shafi, JHEP **1311**, 173 (2013).

[34] S. P. Martin and M. T. Vaughn, Phys. Rev. D **50**, 2282 (1994) [Erratum-ibid. D **78**, 039903 (2008)].

[35] I. Gogoladze, M. U. Rehman and Q. Shafi, Phys. Rev. D **80**, 105002 (2009).